06

Structural changes of multiwalled carbon nanotubes during chemical vapor deposition processes

© I.V. Vilkov[1], A.M. Ob'edkov[1], N.M. Semenov[1], O.A. Kushnerova[1], V.A. Dodonov[1], D.A. Tatarskiy[2]

[1] Razuvaev Institute of Organometallic Chemistry, Russian Academy of Sciences, Nizhny Novgorod, Russia
[2] Lobachevsky University of Nizhny Novgorod, Nizhny Novgorod, Russia
E-mail: mr.vilkof@yandex.ru

Received December 8, 2025
Revised January 10, 2026
Accepted January 21, 2026

The heating processes associated with chemical vapor deposition of nanocoatings during the formation of hybrid nanomaterials based on multiwalled carbon nanotubes can cause structural changes in the nanotubes. Their thermal stability has been determined to be up to 500 °C. At higher temperatures, oxidation of both the nanotubes themselves and catalytic impurities, as well as annealing of defects and graphitization of amorphous carbon forms, are observed. The structure and composition of the nanotubes before and after annealing were studied using electron microscopy, X-ray diffraction analysis, and Raman spectroscopy.

Keywords: annealing, multi walled carbon nanotubes, CVD, thermogravimetric analysis, crystal defects.

DOI: 10.61011/TPL.2026.05.63289.20592

Multiwall carbon nanotubes (MWCNT) play a special role in modern materials science due to a combination of unique mechanical, electrical and thermal properties. However, their applications are limited due to surface inertness, susceptibility to agglomeration and insufficient functionality for specific areas such as catalysis [1], sensorics [2] or structural composites [3,4]. MWCNT surface decoration with metal-containing nanocoatings applied via chemical vapor deposition techniques, in particular, metal-organic chemical vapour deposition (MOCVD), is the most promising technique for surface property control [5–8]. For example, hybrid WC/MWCNT materials are used to create high-strength aluminium matrix composites [6]. WC nanocoating with a thickness of about 20 nm was formed via the MOCVD process using $W(CO)_6$, it plays a key role in transferring induced microstresses from the Al matrix to MWCNT [8]. ZrC/MWCNT [7] that can be used in ceramic ZrO−MWCNT composites is another example of hybrid nanomaterials formed using the MOCVD technique [9].

MOCVD is an effective approach to creating hybrid nanomaterials, however, requires thorough optimization of deposition parameters. Temperature is a key one among them. It affects surface reaction kinetics, reagent diffusion, growth rate and finally structural perfection and functionality of a hybrid nanomaterial. MOCVD precursors have various activation energies, therefore different temperature conditions are required. For example, for formation of WC nanocoatings from $W(CO)_6$, the pyrolysis temperature is only 300 °C [6], while for ZrC deposition from Cp_2ZrCl_2 [7], the best temperature is 900 °C. For SiC deposition from methyl-trichlorosilane, at least 1300 °C is required [10]. MWCNT is a thermodynamically metastable allotropic modification of carbon, they are prone to structural changes and even degradation at high temperatures, in particular, in the presence of chemically active media. Thus, MOCVD synthesis conditions for hybrid nanocoating−MWCNT materials turn out to be limited from below by coating quality requirements and from above by thermochemical stability of MWCNT.

There are several significant studies in the field of temperature stability of carbon nanotubes in air. Thus, the influence of the type of MWCNT growth catalyst on carbon nanotube combustion temperature has been studied in detail by the authors of [11]. They have detected that the oxidation onset temperature in a series of Ni−Co−Fe-based catalysts increased from 325 C to 500 °C. According to comparative analysis of thermal properties of various allotropic forms of carbon [12], MWCNT have demonstrated an intermediate stability between diamond and graphite. It is also known that corona discharge in N_2 can influence a MWCNT structure, forming crystal defects until total failure and amorphization of the surface structure [13]. Thermogravimetric analysis (TGA) in this case has shown a decrease in mass by 7% during heating to 900 °C after discharge processing, which was caused by loss of −N-radicals and sublimation of carbon in the amorphous state. Possible violation of structural integrity of MWCNT during MOCVD is a serious and underexplored issue, which is particularly important for further use of such hybrid nanomaterials.

MWCNT were synthesized via the MOCVD process at atmospheric pressure in argon flow using a technique described in [5]. Toluene and ferrocene served as precursors. For detecting structural changes, MWCNT were annealed in inert atmosphere of 5.5N Ar at atmospheric pressure in a MOCVD reactor. Accurately weighed 100 mg of MWCNT was placed into the reactor. After reactor purging, 100 cm^3/min Ar flow was created and

heating was actuated. Annealing time after reaching the desired temperature was 1 h in each experiment. After complete cooling in Ar flow, samples were removed from the reactor and comprehensively analyzed. TGA was performed in a temperature range of 50–1000 °C on the Pyris 6 TGA (PerkinElmer) thermogravimetric analyzer in oxidizing atmosphere (zero gas — A grade air) or in inert atmosphere of Ar (5.5N), heating rate was 5 °C/min. Phase composition of the samples was determined by the X-ray diffraction analysis (XPA) on the Tongda TD-3700 diffractometer using ICDD PDF-4+ 2014 powder diffraction database (hereinafter referred to as PDF).

The MWCNT structure was examined before and after annealing using the transmission electron microscopy (TEM) on the Jeol JEM 2000EX and high-resolution transmission electron microscopy (HRTEM) on the Zeiss Libra 200MC. Samples were subjected to ultrasonic dispersion in isopropyl alcohol during 30 min, and then deposited onto copper grids with carbon substrates.

MWCNT were studied by the Raman-scattering spectroscopy using the NTEGRA Spectra (NT-MDT) research platform, 473 nm laser, power not higher than 50 mW. Raman scattering spectra were measured in a range of 150–3200 cm^{-1}.

As can be seen from the TGA/DTG curves (DTG — differential thermogravimetry) (Figure 1), initial MWCNT demonstrated stability during heating in air to 480 °C, maximum rate of mass loss according to the rate curve (dW/dT) was reached at 582 °C, the process ended at 650 °C, residue in the form of Fe_2O_3 was 4.7 mass%. Combustion of initial MWCNT in air according to DTG takes place in one stage, however, early loss of mass within 3 mass% from 480 to 500 °C can be attributed to combustion of amorphous forms of carbon [12]. According to isoconversion calculations [14], the oxidation reaction activation energy was 170 ± 5 kJ/mol. Compared with the literature data [12,15–17], the calculated value corresponds

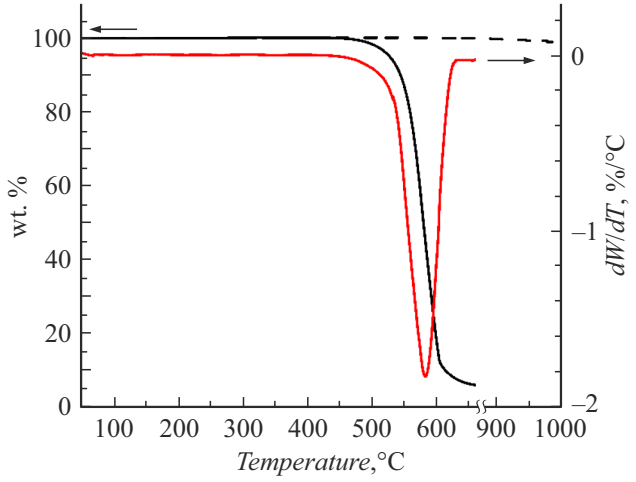

Figure 1. TGA curves (solid curve — in air, dashed curve — in Ar) (left-hand axis), and DTG curve (right-hand axis) for oxidation of initial MWCNT in air.

to MWCNT with a high quality crystal structure. TGA of initial MWCNT was also conducted in inert atmosphere of Ar. Slow loss of 2 mass% was detected in a range from 880 to 1000 °C. Similar loss of mass in a range from 800 to 1280 °C was observed in [17]. The authors attributed that to slow sublimation of amorphous carbon impurities, which could be caused by sublimation of carbon clusters from MWCNT surface and oxygen desorption with concurrent reduction of sp^2-hybrid state of carbon on the surface.

According to the XPA data (Figure 2), initial MWCNT, besides the primary crystal phase corresponding to MWCNT contain impurities in the form of catalytic iron-containing nanoparticles, i. e. γ-Fe phase (PDF N 01-089-4185) and Fe_3C phase (PDF N 00-034-0001). The presence of α-Fe phase (PDF N 00-006-0696) is attributed to a phase transition of some γ-Fe nanoparticles larger than 20 nm. Profile analysis (results are shown in the table in Figure 2) has established that annealing caused MWCNT structure relaxation. This is proved by decreasing interplanar spacing d_{002} from 3.402 Å for initial MWCNT to 3.392 Å for MWCNT annealed at 900 °C. Statistically significant change in FWHM of the (002) peak wasn't detected. After annealing at 900 °C, formation of a small amount of iron(II) oxide (Fe_3O_4) (PDF N 01-088-0866) was found. This is most likely caused by oxidation of Fe_3C and α-Fe, which is proved by a decrease in the intensity of the resultant Fe_3C peak at 38° and by a dip at 44.5° corresponding to α-Fe (110). TGA excludes oxidation with oxygen, because mass gain is not observed at temperatures > 500 °C up to 880 °C. Taking into account a large specific area of MWCNT, oxygen entrapped and chemically bound by surface defects can diffuse, during annealing, along the surface and oxidize Fe_3C and α-Fe, while γ-Fe encapsulated into internal MWCNT channels remains unavailable.

Structural changes of MWCNT samples after annealing were studied using the Raman-scattering spectroscopy technique. According to the results (Figure 3, *a*), annealing at temperatures up to 900 °C doesn't affect positions of *D*-, *G*- and 2*D*-resonance signals, which are detected at 1352 cm^{-1}, 1573 cm^{-1} and 2707 cm^{-1}, respectively [9]. Band *D* refers to defects associated with violation of the MWCNT structure, these are generally dislocations or surface C atoms in a state other than the sp^2-hybrid state. Band *G* corresponds to tangential oscillations in a graphene layer and indicates an ordered crystal structure of carbon in the sp^2-hybrid state. In a range of 150–200 cm^{-1}, a radial breathing mode corresponding to single-walled carbon nanotubes wasn't detected.

To estimate the quality and quantitative characteristic of MWCNT structure, the Tuinstra–Koenig relation, which is defined as the ratio of integral intensities of *D*- and *G*-resonances (I_D/I_G). For samples annealed at temperatures from 100 to 500 °C, it remains almost the same and can be linearly approximated $I_D/I_G = 0.26$ (Figure 3, *b*). Annealing at 750 and 900 °C caused a decrease in I_D/I_G to 0.22 and 0.21, respectively, which indicates that the

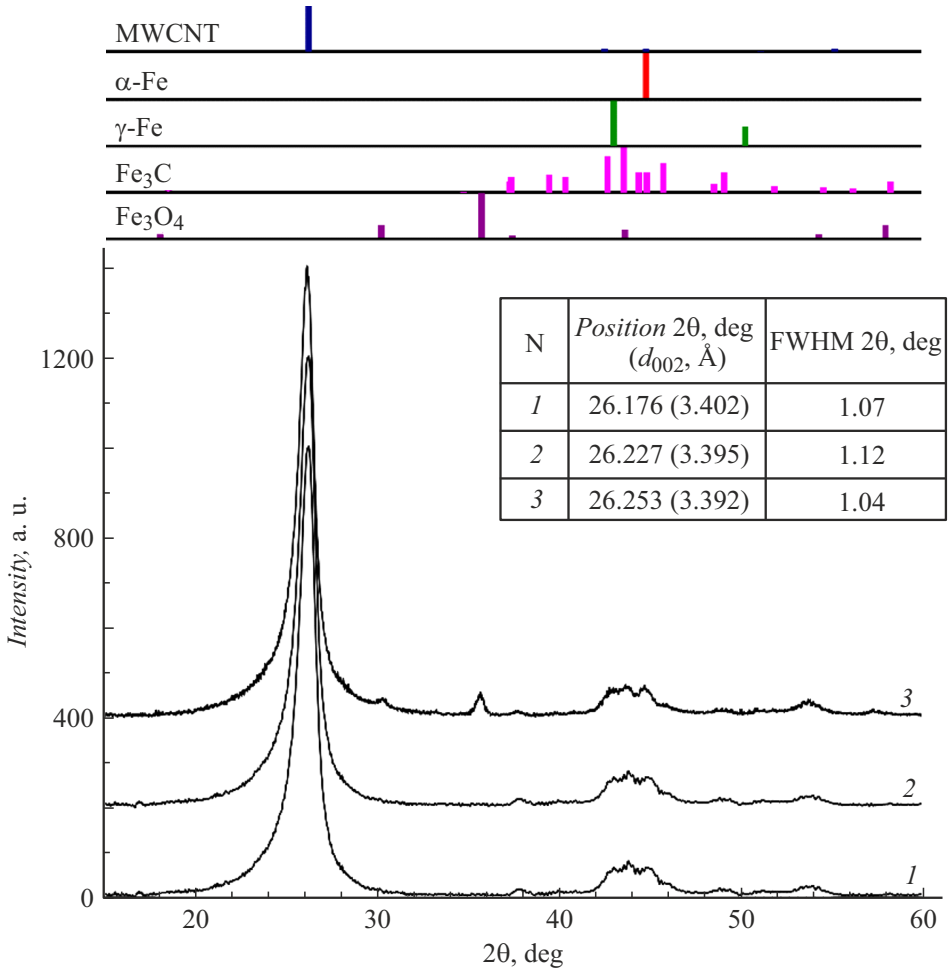

N	*Position* 2θ, deg (d_{002}, Å)	FWHM 2θ, deg
1	26.176 (3.402)	1.07
2	26.227 (3.395)	1.12
3	26.253 (3.392)	1.04

Figure 2. Diffraction patterns of initial MWCNT (*1*) and MWCNT after annealing in inert atmosphere at $T = 500$ (*2*) and 900 °C (*3*).

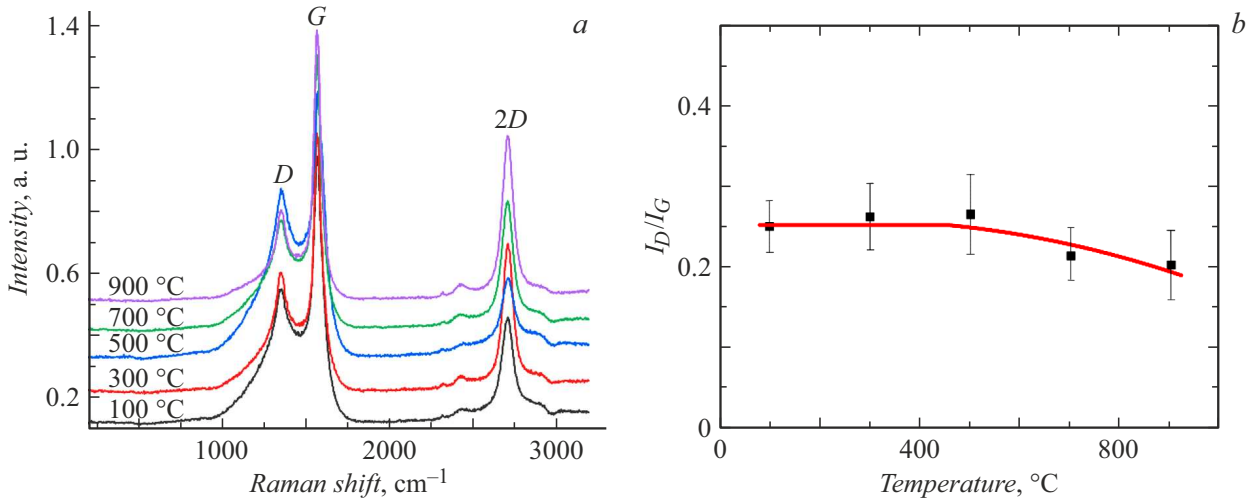

Figure 3. *a* — Raman spectra of MWCNT annealed at various temperatures; *b* — Tuinstra– Koenig relations for MWCNT after annealing in Ar at various temperatures.

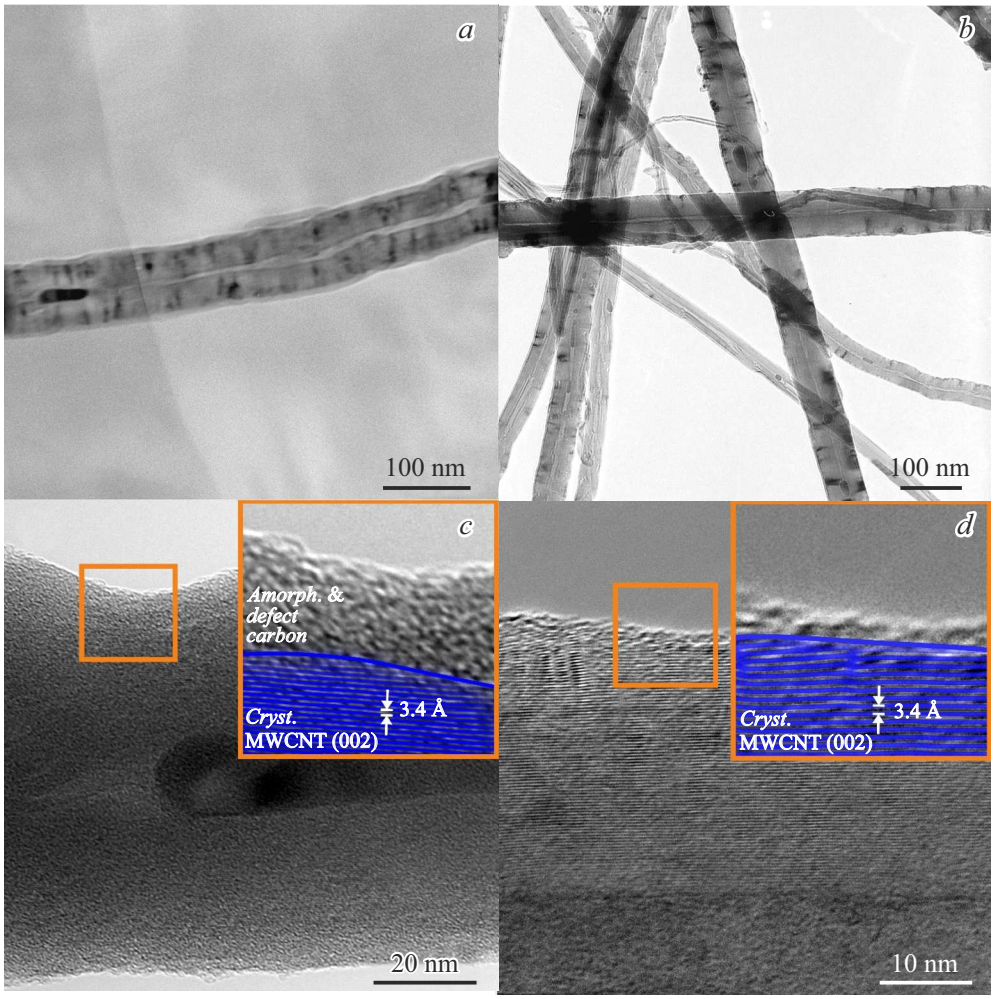

Figure 4. TEM images of MWCNT before annealing (a) and after annealing at 900 °C (b), of HRTEM before (c) and after annealing at 900 °C (d). Insets (c and d) show magnified regions enclosed in a frame in the main figure, with superimposed phase contrast after Fourier filtration — a system of lines corresponding to a system of atomic planes (002).

proportion of defects in the MWCNT structure and amount of amorphous impurities decrease. TEM was able to detect the presence of amorphous defect shell, the results were compared with the data for MWCNT after annealing.

According to the electron microscopy data, initial MWCNT have a mean diameter of 48 nm and a length up to 0.1 mm. Figure 4 clearly shows the presence (a) and the absence (b) of a layer that differs from the MWCNT-specific contrast. This layer does not occur on all initial MWCNT, which indicates that there is a zone of nonuniform conditions appearing during synthesis of initial MWCNT. Thickness of such amorphous layer reaches 10 nm. HRTEM phase contrast techniques (Figure 4, c and d) were able to visualize a MWCNT edge and detect the amorphous layer. Interplanar spacing in the [002] direction was 3.4 Å, which agrees with XPA data taking into account the instrument error.

Despite an apparent rigidity of the MWCNT structure, MWCNT turn out to be very chemically and structurally active in a temperature range corresponding to MOCVD. This is primarily associated with the presence of an amorphous surface carbon layer with a thickness up to ~ 10 nm, which partially sublimes and gets graphitized when heated to ~ 900 °C, and becomes more ordered. Decrease in the interplanar spacing in the [002] direction and decrease in I_D/I_G are indicative of relaxation of the MWCNT crystal structure. Taken together, this indicates that the degree of ordering of the MWCNT structure increases due to defect annealing and reduction of the amorphous component.

Such behavior directly affects the deposition processes in MOCVD and in related gas phase techniques. First, surface layer restructuring modifies the density and form of nucleation centers, which can cause a change in morphology and distribution of nanoparticles and nanocoatings on the MWCNT surface. Second, sublimation and/or decomposition of amorphous carbon at high temperatures make MWCNT an additional source of carbon in the reactor, which can change the effective precursor ratio and composition of the deposited phase. Finally, defects induced by the deposition process itself can partially relax

as early as at the high-temperature process stage, therefore ex post facto analysis (for example, using Raman-scattering spectroscopy data) can underestimate the real structural damage. All these factors shall be considered when choosing MOCVD conditions and interpreting the results of deposition on MWCNT.

Acknowledgments

The study used equipment provided by shared research facilities: Analytical Center of the Institute of Organometallic Chemistry, Russian Academy of Sciences, and Physics and Technology of Microstructures and Nanostructures of the Institute for Physics of Microstructures, Russian Academy of Sciences.

Funding

The study was carried out as part of project No. 25-23-20235 of the Russian Science Foundation.

Conflict of interest

The authors declare no conflict of interest.

References

[1] M.T. Tourchi Moghadam, M. Seifi, M.B. Askari, S. Azizi, J. Phys. Chem. Solids, **165**, 110688 (2022). DOI: 10.1016/J.JPCS.2022.110688
[2] R. Lozano-Rosas, J.M. Bravo-Arredondo, V.K. Karthik-Tangirala, M.J. Robles-Águila, Appl. Phys. A, **129**, 788 (2023). DOI: 10.1007/S00339-023-07061-7
[3] V. Srinivasan, S. Kunjiappan, P. Palanisamy, Int. Nano Lett., **11**, 321 (2021). DOI: 10.1007/S40089-021-00328-Y
[4] K. Ramachandran, V. Boopalan, J.C. Bear, R. Subramani, J. Mater. Sci., **57**, 3923 (2021). DOI: 10.1007/S10853-021-06760-X
[5] I.V. Vilkov, B.S. Kaverin, A.M. Ob'edkov, N.M. Semenov, S.Yu. Ketkov, E.A. Rychagova, S.A. Gusev, D.A. Tatarskiy, P.V. Andreev, A.V. Aborkin, Mater. Today Chem., **24**, 100830 (2022). DOI: 10.1016/J.MTCHEM.2022.100830
[6] I.V. Vilkov, A.M. Ob'edkov, S.Yu. Ketkov, N.M. Semenov, B.S. Kaverin, R.S. Kovylin, A.V. Aborkin, K.E. Smetanina, Tech. Phys. Lett., **49** (6), 77 (2023). DOI: 10.61011/TPL.2023.06.56387.19534.
[7] I.V. Vilkov, A.M. Ob'edkov, B.S. Kaverin, N.M. Semenov, R.S. Kovylin, V.A. Dodonov, Russ. J. Gen. Chem., **93**, S844 (2023). DOI: 10.1134/S1070363223160247
[8] A. Aborkin, D. Bokaryov, D. Babin, A. Zalesnov, K. Khorkov, E. Prusov, A. Elkin, A. Ob'edkov, I. Vilkov, I. Perezhogin, M. Alymov, Ceram. Int., **49**, 4785 (2023). DOI: 10.1016/j.ceramint.2022.09.368
[9] A.A. Leonov, E.V. Abdulmenova, M.P. Kalashnikov, Inorg. Mater. Appl. Res., **12**, 482 (2021). DOI: 10.1134/S2075113321020313
[10] K.I. Park, J.H. Kim, H.K. Lee, D.K. Kim, Mod. Phys. Lett. B, **23**, 3877 (2011). DOI: 10.1142/S0217984909021946
[11] G.S.B. McKee, K.S. Vecchio, J. Phys. Chem. B, **110**, 1179 (2005). DOI: 10.1021/JP054265H
[12] F. Cataldo, Fulleren. Nanotub. Carbon Nanostruct., **10**, 293 (2002). DOI: 10.1081/FST-120016451
[13] L. Xu, Z. Fang, P. Song, M. Peng, Appl. Surf. Sci., **256**, 6447 (2010). DOI: 10.1016/J.APSUSC.2010.04.033
[14] A.A. Jain, A. Mehra, V.V. Ranade, Fuel, **165**, 490 (2016). DOI: 10.1016/J.FUEL.2015.10.042
[15] L. De Ferreira, F.S. Medeiros, B.C.R. Araujo, M.S. Gomes, M.L. Rocco, R.C.O. Sebastião, H.D.R. Calado, Thermochim. Acta, **676**, 145 (2019). DOI: 10.1016/J.TCA.2019.03.040
[16] Y.C. Hsieh, Y.C. Chou, C.P. Lin, T.F. Hsieh, C.M. Shu, Aerosol Air Qual. Res., **10**, 212 (2010). DOI: 10.4209/AAQR.2009.08.0053/METRICS
[17] A. Mahajan, A. Kingon, A. Kukovecz, Z. Konya, P.M. Vilarinho, Mater. Lett., **90**, 165 (2013). DOI: 10.1016/J.MATLET.2012.08.120

Translated by E.Ilyinskaya